

$^{169}\text{Tm}(n, \gamma)$ Cross Section and Statistical γ Decay Properties from DANCE Measurements*

*I. Knapová¹, K. Horčíčková², A. Couture¹, C. Fry¹, F. Gunsing³, T. Kawano¹,
K. J. Kelly¹, M. Krtyčka², E. Leal Cidoncha¹, C. J. Prokop¹, R. Reifarth¹,
G. Rusev¹, J. L. Ullmann¹, S. Valenta²*

¹Los Alamos National Laboratory


²Institute of Particle and Nuclear Physics, Charles University, Prague

³CEA Irfu, Université Paris-Saclay

Oslo Workshop, May 2026

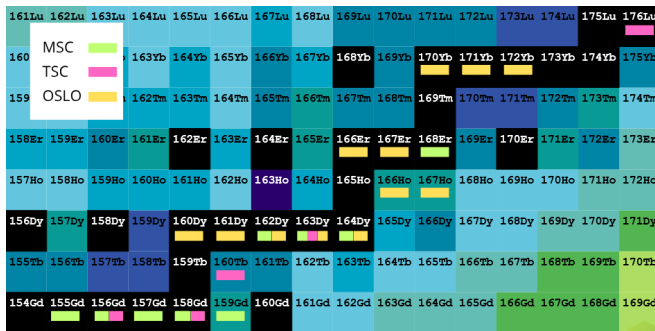
Funding acknowledgments

This work is supported by Charles Uni. Research Centre program No. UNCE/24/SCI/016 and GAČR grant No. 23-06439S of the Czech Sci. Fdn. It also benefits from the use of the LANSCE and is supported by the US DoE through the LANL. LANL is operated by Triad National Security, LLC, for the NNSA of US DoE (Contract No. 89233218CNA000001). This presentation was supported by Grant Agency of Charles Uni. project No. 428726.

*I. Knapová, K. Horčíčková, et al. In: *Phys. Rev. C* 112 (2025), p. 014612 

Why Thulium?

- Thulium - monoisotopic rare-earth element
- diagnostic tool for monitoring neutron flux
- astrophysical interest: nuclei synthesis around $A = 170$
- systematic study of the PSFs and LD in the region

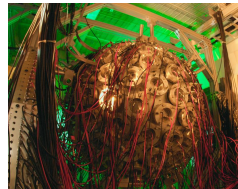


Experiment

- data from Los Alamos National Laboratory (LANL)

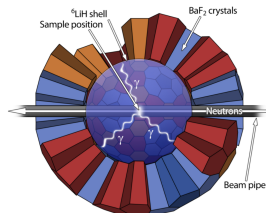


- Detector for Advanced Neutron Capture Experiments (DANCE)



Experiment

- measuring $^{169}\text{Tm}(n, \gamma)$
- neutron resonances: $J^\pi = 0^+, 1^+$
- DANCE:
 - 160 BaF_2 scintillation crystals
 - 20.25 m from the spallation target
 - covers $\approx 3.5 \pi$ solid angle



cut through DANCE detector

- neutrons produced in a spallation reaction of 800-MeV protons striking a tungsten target
- neutron energies from sub-thermal to units of MeV

Two parts of the analysis:

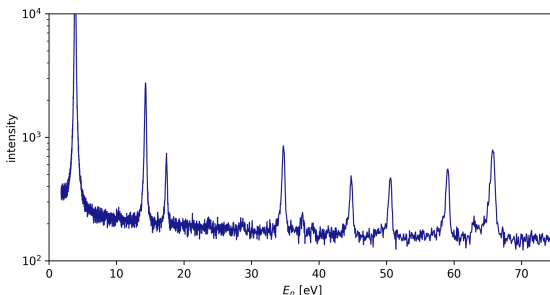
1. Kamila – Photon Strength Functions (PSFs)
 - compound nucleus $^{169}\text{Tm}+n$
 - coincidence γ -ray spectra
 - collective states impact: scissors mode (SM)

Two parts of the analysis:

1. Kamila – Photon Strength Functions (PSFs)
 - compound nucleus $^{169}\text{Tm}+n$
 - coincidence γ -ray spectra
 - collective states impact: scissors mode (SM)
2. Ingrid – cross-section
 - cross-section of reaction $^{169}\text{Tm}(n, \gamma)$
 - deduce MACS
 - calculate astrophysical impact, change of abundances

Two parts of the analysis:

1. Kamila – Photon Strength Functions (PSFs)
 - compound nucleus $^{169}\text{Tm}+n$
 - coincidence γ -ray spectra
 - collective states impact: scissors mode (SM)
2. Ingrid – cross-section
 - cross-section of reaction $^{169}\text{Tm}(n, \gamma)$
 - deduce MACS
 - calculate astrophysical impact, change of abundances



Basics of data processing

Each event is characterized by

1. neutron energy
2. detected multiplicity
3. deposited γ energies

→ event-by-event sorting into various spectra

Basics of data processing

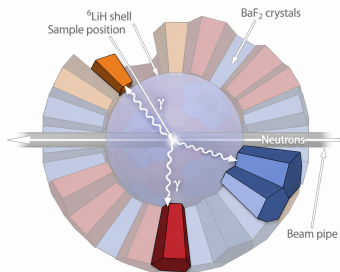
Each event is characterized by

1. neutron energy
2. detected multiplicity
3. deposited γ energies

→ event-by-event sorting into various spectra

- neutron energies by the time-of-flight (TOF) method
- all signals detected within a preset coincidence window of 10 ns → one event
- all *neighboring* signals^a form a cluster
- number of clusters: detected multiplicity M

^aone γ ray may deposit energy in several detectors → clusterization



Multi-Step γ -ray Cascade spectra

MSC spectra are created from events

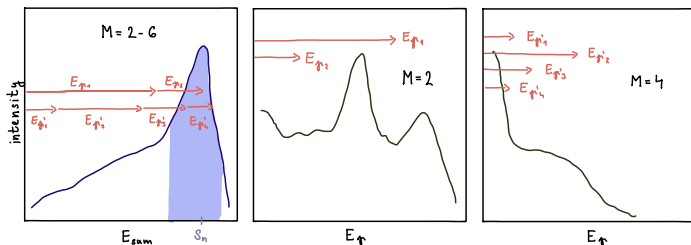
- with total deposited energy in narrow interval around $S_n = 6.592$ MeV (energy released in neutron capture)
- corresponding to strong, well-separated resonances
- sorted by multiplicity M (\leftarrow good estimate of # of γ -rays)

Multi-Step γ -ray Cascade spectra

MSC spectra are created from events

- with total deposited energy in narrow interval around $S_n = 6.592$ MeV (energy released in neutron capture)
- corresponding to strong, well-separated resonances
- sorted by multiplicity M (\leftarrow good estimate of # of γ -rays)

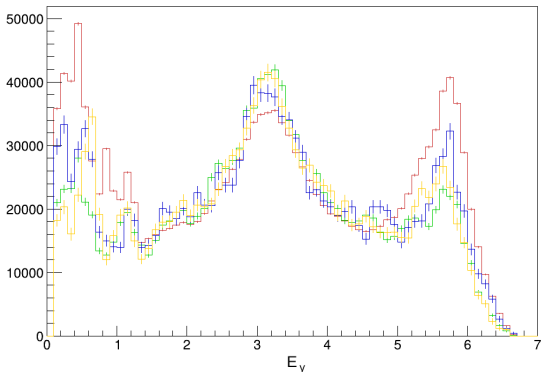
MSC spectra are distribution of E_γ for each M



19 $J^\pi = 1^+$ and 6 $J^\pi = 0^+$ resonances \rightarrow average spectra for each spin group

MSC spectra

- Porter-Thomas fluctuations \Rightarrow spectra from individual resonances slightly different, but show similar features
- between spin groups statistically significant differences but again similar features



MSC spectra of few 1^+ resonances, $M = 2$

Simulations

- MSC spectra – complicated interplay of PSFs, LD and detector response
- unrealistic to directly extract information on LD and PSFs from experimental spectra

Simulations

- MSC spectra – complicated interplay of PSFs, LD and detector response
- unrealistic to directly extract information on LD and PSFs from experimental spectra
- check of theoretical assumptions: *trial-and-error* comparison of experimental and simulated spectra
- matching of sum-energy spectra important for detection efficiency estimation → essential for cross-section analysis

- MSC spectra – complicated interplay of PSFs, LD and detector response
- unrealistic to directly extract information on LD and PSFs from experimental spectra
- check of theoretical assumptions: *trial-and-error* comparison of experimental and simulated spectra
- matching of sum-energy spectra important for detection efficiency estimation → essential for cross-section analysis

1. Monte Carlo simulations of γ cascades: DICEBOX algorithm¹

¹F. Bečvář. In: *Nucl. Instrum. Methods A* 417 (1998), pp. 434–449

Simulations

- MSC spectra – complicated interplay of PSFs, LD and detector response
- unrealistic to directly extract information on LD and PSFs from experimental spectra
- check of theoretical assumptions: *trial-and-error* comparison of experimental and simulated spectra
- matching of sum-energy spectra important for detection efficiency estimation → essential for cross-section analysis

1. Monte Carlo simulations of γ cascades: DICEBOX algorithm¹
2. GEANT4 simulation^{2,3} of the detector response

¹F. Bečvář. In: *Nucl. Instrum. Methods A* 417 (1998), pp. 434–449

²S. Agostinelli et al. In: *Nucl. Instrum. Methods A* 506 (2003), pp. 250–303

³M. Jandel et al. In: *Nucl. Instrum. Methods B* 261 (2007), pp. 1117–1124 

- MSC spectra – complicated interplay of PSFs, LD and detector response
 - unrealistic to directly extract information on LD and PSFs from experimental spectra
 - check of theoretical assumptions: *trial-and-error* comparison of experimental and simulated spectra
 - matching of sum-energy spectra important for detection efficiency estimation → essential for cross-section analysis
1. Monte Carlo simulations of γ cascades: DICEBOX algorithm¹
 2. GEANT4 simulation^{2,3} of the detector response
 3. compare spectra, assess compatibility, rinse and repeat

¹F. Bečvář. In: *Nucl. Instrum. Methods A* 417 (1998), pp. 434–449

²S. Agostinelli et al. In: *Nucl. Instrum. Methods A* 506 (2003), pp. 250–303

³M. Jandel et al. In: *Nucl. Instrum. Methods B* 261 (2007), pp. 1117–1124 

The following are available for odd-odd compound:

- PSF parameters from Oslo analysis $^{166}\text{Ho}^1$
 - SM at 3.14 MeV
 - strength $4.2 \mu_N^2$
- ^{160}Tb TSC analysis²
 - SM at 2.6 MeV
 - strength $6(1) \mu_N^2$

¹F. Pogliano et al. In: *Phys. Rev. C* 107 (2023), p. 034605

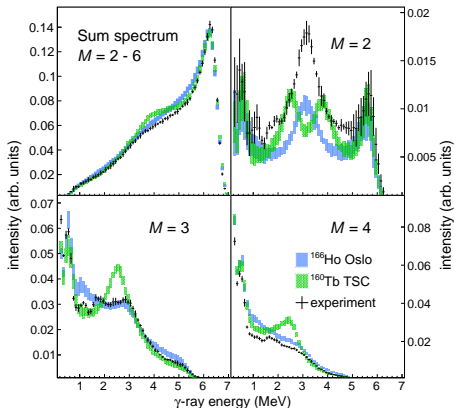
²J. Kroll et al. In: *Int. J. Mod. Phys. E* 20 (2011), pp. 526–531

Models from literature

The following are available for odd-odd compound:

- PSF parameters from Oslo analysis $^{166}\text{Ho}^1$
 - SM at 3.14 MeV
 - strength $4.2 \mu_N^2$
- ^{160}Tb TSC analysis²
 - SM at 2.6 MeV
 - strength $6(1) \mu_N^2$
- global calculations from IAEA PSFs database: D1M-QRPA, SMLO

→ unsatisfactory description



¹F. Pogliano et al. In: *Phys. Rev. C* 107 (2023), p. 034605

²J. Kroll et al. In: *Int. J. Mod. Phys. E* 20 (2011), pp. 526–531

Search for an optimal model

We have run hundreds of simulations to scan parameter space for several model combinations of PSFs and LD.

Search for an optimal model

We have run hundreds of simulations to scan parameter space for several model combinations of PSFs and LD.

PSF requirements:

- major impact of the scissors mode (SM) on the γ decay
- sensitivity to the transition multipolarity – SM in $M1$
- SM energy at about 3.3 MeV (surely in 3.0-3.5 MeV)
- other resonances in PSFs – spin-flip ($M1$), Pygmy ($E1$)
- no sizable upbend in dipole PSF
- not sensitive to $E2$ and higher PSFs

Search for an optimal model

We have run hundreds of simulations to scan parameter space for several model combinations of PSFs and LD.

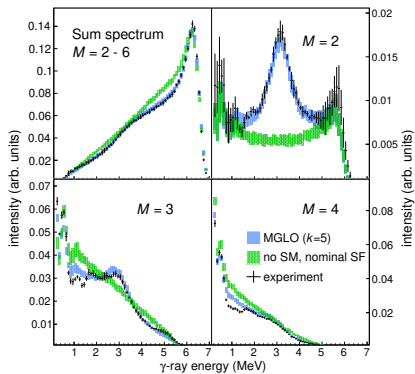
PSF requirements:

- major impact of the scissors mode (SM) on the γ decay
- sensitivity to the transition multipolarity – SM in $M1$
- SM energy at about 3.3 MeV (surely in 3.0-3.5 MeV)
- other resonances in PSFs – spin-flip ($M1$), Pygmy ($E1$)
- no sizable upbend in dipole PSF
- not sensitive to $E2$ and higher PSFs

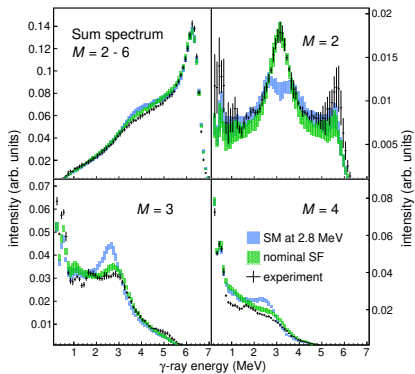
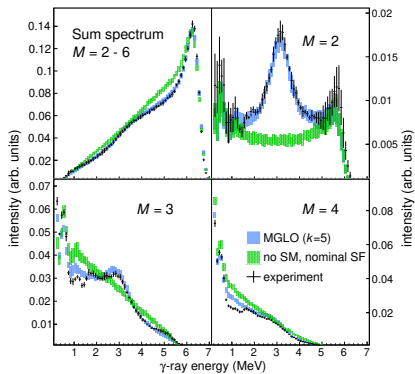
Level Density conclusions:

- BSFG model preferred w.r.t. CT or microscopical HFB
- no indication of parity asymmetry or other fine effects

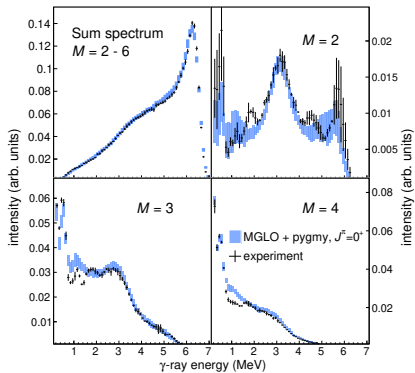
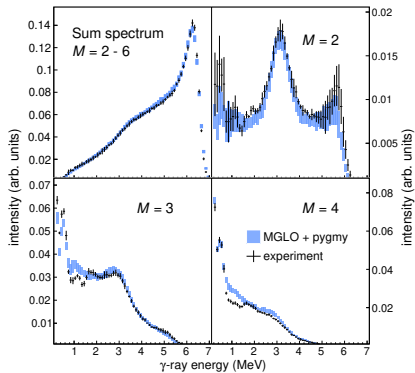
Search for an optimal model



Search for an optimal model



Consistency for both resonance spins



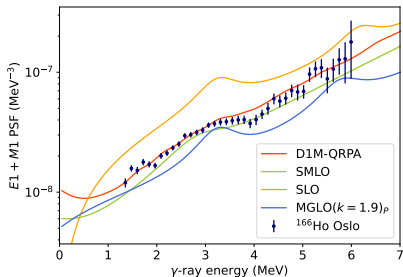
Best description

- MGLO¹ $E1$ PSF model proposed by our group
- SM at 3.3 MeV, width 1.0 MeV, strength $6(1) \mu_N^2$
- double-bump spin-flip at 6.2 MeV and 7.7 MeV in $M1$
- Pygmy resonance at 5.8 MeV in $E1$

¹J. Kroll et al. In: *Phys. Rev. C* 88 (2013), p. 034317

Best description

- MGLO¹ *E1* PSF model proposed by our group
- SM at 3.3 MeV, width 1.0 MeV, strength $6(1) \mu_N^2$
- double-bump spin-flip at 6.2 MeV and 7.7 MeV in *M1*
- Pygmy resonance at 5.8 MeV in *E1*

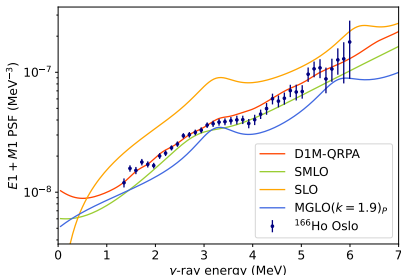


- other *E1* PSFs giving acceptable description: KMF, SLO

¹J. Kroll et al. In: *Phys. Rev. C* 88 (2013), p. 034317

Total radiative width

- MSC are not sensitive to the absolute scale of PSFs, total radiative width $\bar{\Gamma}_\gamma$ is the only quantity which is sensitive
- value from the literature ENDF/B-VII.0: $\bar{\Gamma}_\gamma = 86$ meV
- MGLO $E1$ PSF parametrized to reproduce this value



model comb.	$\bar{\Gamma}_\gamma$ (meV)	
	$J^\pi = 0^+$	$J^\pi = 1^+$
SLO	231(5)	
MGLO($k=1.9$) _p	92(2)	
KMF	90.5(15)	
D1M-QRPA	37.2(35)	175(5)
SMLO	30.9(26)	146(4)

Cross-section

Measured for energies between 1.8 eV to 0.97 MeV using 2 samples (thin and thick) with $n = 6.9 \times 10^{-6}$ and 1.7×10^{-4} atoms/b.

Cross-section

Measured for energies between 1.8 eV to 0.97 MeV using 2 samples (thin and thick) with $n = 6.9 \times 10^{-6}$ and 1.7×10^{-4} atoms/b.

- both samples allow thin-sample approximation

$$\sigma(E_n) = \frac{1}{nS} \frac{C(E_n) - B(E_n)}{\varepsilon(E_n) \phi(E_n)}$$

Cross-section

Measured for energies between 1.8 eV to 0.97 MeV using 2 samples (thin and thick) with $n = 6.9 \times 10^{-6}$ and 1.7×10^{-4} atoms/b.

- both samples allow thin-sample approximation

$$\sigma(E_n) = \frac{1}{nS} \frac{C(E_n) - B(E_n)}{\varepsilon(E_n) \phi(E_n)}$$

- corrected for self-attenuation effects and ^{181}Ta contribution
- neutron flux measured by beam monitors

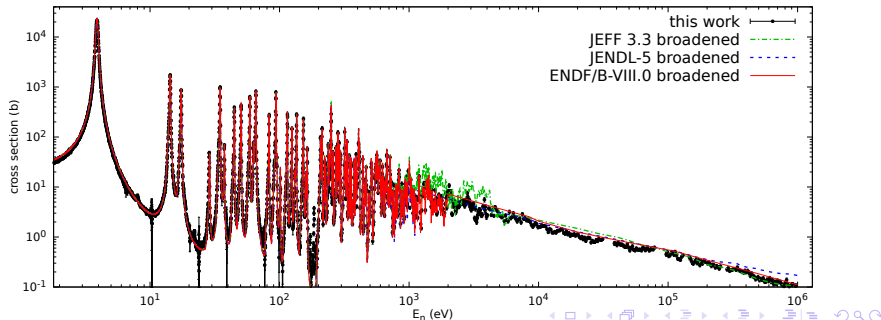
Cross-section

Measured for energies between 1.8 eV to 0.97 MeV using 2 samples (thin and thick) with $n = 6.9 \times 10^{-6}$ and 1.7×10^{-4} atoms/b.

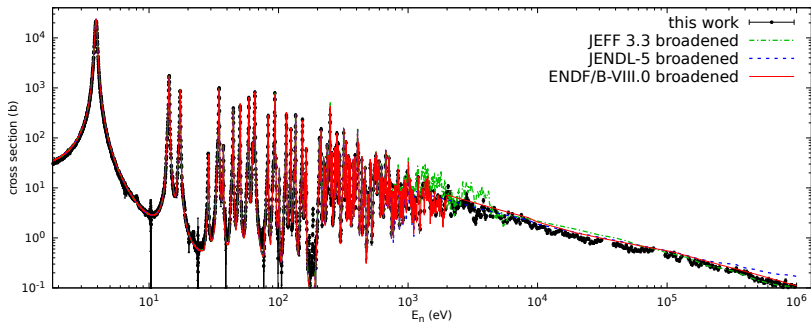
- both samples allow thin-sample approximation

$$\sigma(E_n) = \frac{1}{nS} \frac{C(E_n) - B(E_n)}{\varepsilon(E_n) \phi(E_n)}$$

- corrected for self-attenuation effects and ^{181}Ta contribution
- neutron flux measured by beam monitors



Comparison with evaluations



- up to ≈ 700 keV all almost identical, good description
- in RRR above 1 keV ENDF/B-VIII.0 agrees best
- in URR largest discrepancy between 10 and 100 keV
- above 100 keV JEFF 3.3 consistent, ENDF/B-VIII.0 slightly and JENDL-5 considerably higher

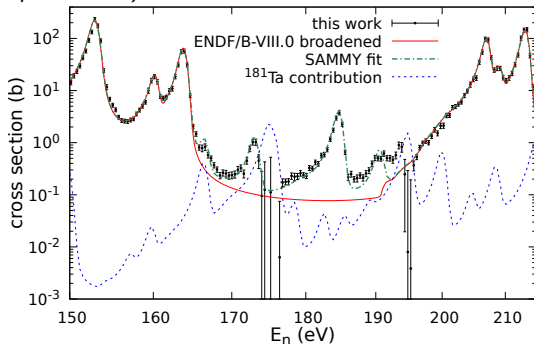
New resonances

- altogether eight new resonances
- energy and $g\Gamma_n$ estimation by SAMMY fit with $\Gamma_\gamma = 86$ meV (average Γ_γ from ENDF/B-VIII.0)

New resonances

- altogether eight new resonances
- energy and $g\Gamma_n$ estimation by SAMMY fit with $\Gamma_\gamma = 86$ meV (average Γ_γ from ENDF/B-VIII.0)

E_R (eV)	$g\Gamma_n$ (meV)
8.037(6)	0.00072(4)
22.03(1)	0.00141(6)
71.85(2)	0.0136(7)
75.57(2)	0.0199(8)
166.46(4)	0.055(8)
173.07(5)	0.086(12)
184.69(2)	0.316(8)
190.61(4)	0.056(3)



new resonance structures at $E_n = 170 - 200$ eV

Astrophysical implications

- Maxwellian-averaged capture cross-section (MACS)

$$\sigma_{MACS}(k_B T) = \frac{2}{\sqrt{\pi}} \left(\frac{\mu}{k_B T} \right)^2 \int_0^\infty \sigma(E_n) E_n e^{-\frac{E_n}{k_B T}} d(E_n)$$

- direct impact on astrophysical nucleosynthesis reaction rates

¹M. Weigand et al. In: *Phys. Rev. C* 92 (2015), p. 045810

Astrophysical implications

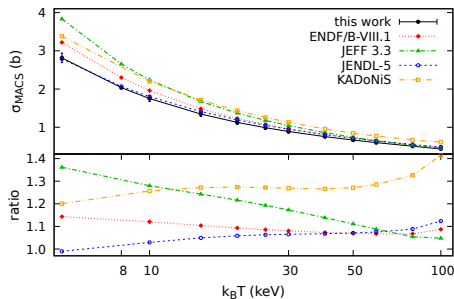
- Maxwellian-averaged capture cross-section (MACS)

$$\sigma_{MACS}(k_B T) = \frac{2}{\sqrt{\pi}} \left(\frac{\mu}{k_B T} \right)^2 \int_0^\infty \sigma(E_n) E_n e^{-\frac{E_n}{k_B T}} d(E_n)$$

- direct impact on astrophysical nucleosynthesis reaction rates

s-process simulation network with NETZ¹:

- ¹⁶⁹Tm abundance increase by 26 %
- changes of the abundances of elements heavier than ¹⁶⁹Tm are in the order of 0.2 %

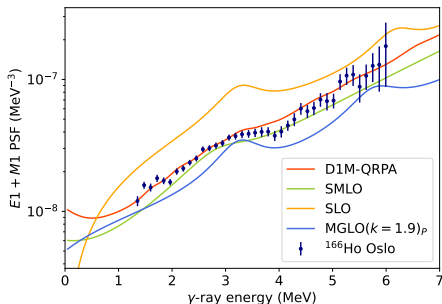


MACS numerically integrated for $k_B T = 5 - 100$ keV

¹M. Weigand et al. In: *Phys. Rev. C* 92 (2015), p. 045810

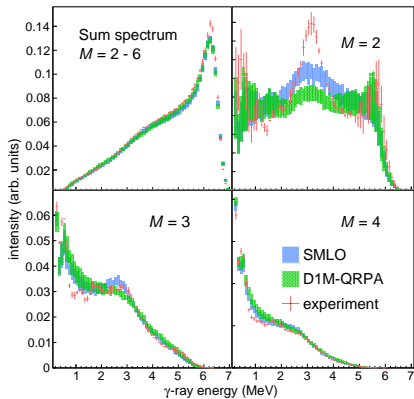
Conclusions

- disagreement of experimental data and previously proposed PSF models
- most successful $E1$ PSF model: MGLO
- necessary to include: SM, SF, and Pygmy
- BSFG level density model preferred

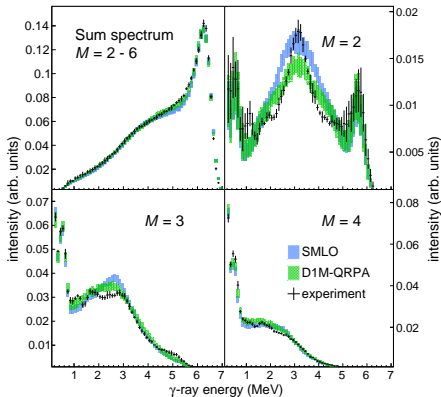


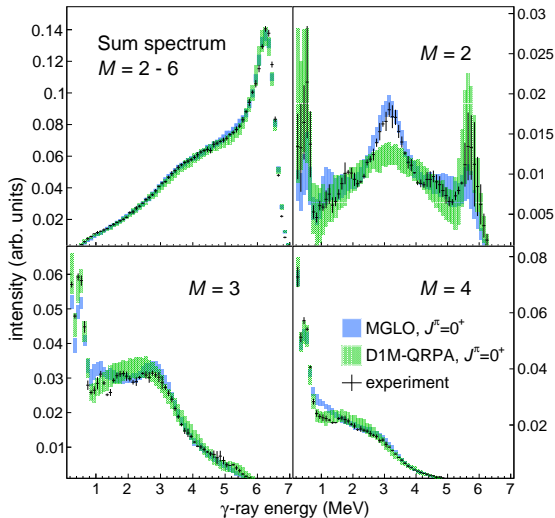
- cross-section measured from 1.8 eV to 0.97 MeV

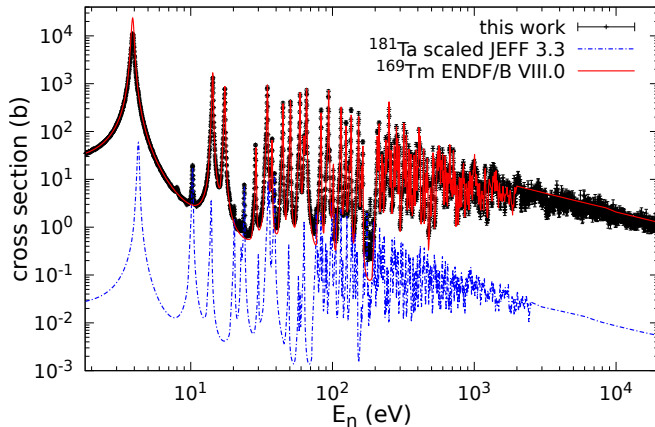
BSFG LD model



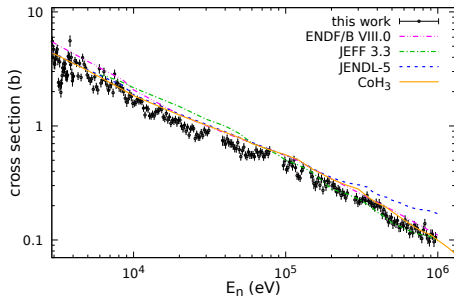
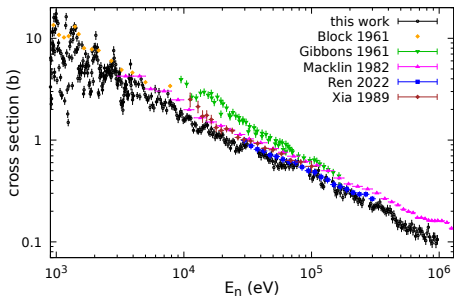
HFB microscopic LD model



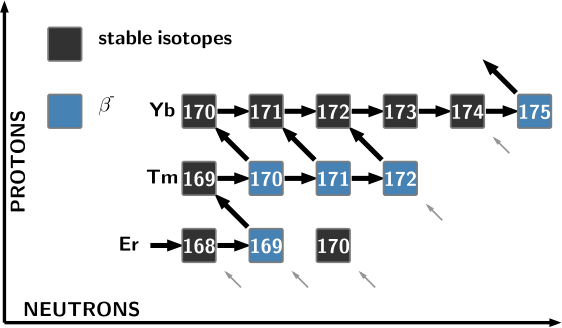
D1M-QRPA $J^\pi = 0^+$ 

^{181}Ta impurity

URR

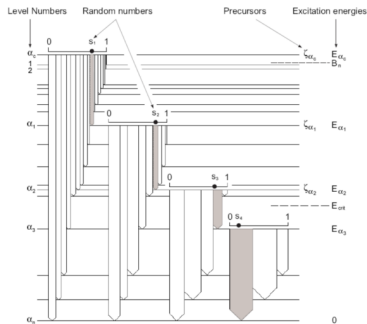


s-process



Back-up – simulations of γ cascades

- various PSF and LD model parameters as input
- validity of the statistical model of γ decay above $E_{\text{crit}} = 960$ keV
- individual radiative width properties:
 - statistically independent
 - follow the Porter-Thomas (PT) distribution
- impact of PT fluctuations - 20 different artificial nuclei
- within each artificial nucleus 10^5 cascades
- below E_{crit} : decay scheme from ENSDF¹



¹C. M. Baglin et al. In: *Nucl. Data Sheets* 153 (2018), pp. 1–494.

correlation matrix for simulated MSC spectra

